

Article

Halloysite Nanotubes as Adsorptive Material for Phosphate Removal from Aqueous Solution

Hermin Saki ¹, Esayas Alemayehu ², Joachim Schomburg ³ and Bernd Lennartz ^{1,*} 

¹ Faculty of Agricultural and Environmental Sciences, University of Rostock, Justus-von-Liebig-Weg 6, 18059 Rostock, Germany; hermin.saki@uni-rostock.de

² Faculty of Civil & Environmental Engineering, Jimma University, Jimma 378, Ethiopia; esayas16@yahoo.com

³ Durtec GmbH, Genzkower Strasse 7, 17034 Neubrandenburg, Germany; info@durtec-gmbh.de

* Correspondence: bernd.lennartz@uni-rostock.de; Tel.: +49-381-498-3180

Received: 30 November 2018; Accepted: 21 January 2019; Published: 24 January 2019



Abstract: In this study, we were aiming at testing halloysite nanotubes as an efficient adsorbent for the removal of phosphate from agricultural runoff. Adsorption of phosphate onto powder and granular form of halloysite nanotubes has been examined by using the classical batch method and diffusion experiments at room temperature. Different forms of halloysite nanotubes were investigated to explore the effect of structure on the adsorption of phosphate. The maximum adsorption efficiency was obtained for powder halloysite nanotubes (79.5%) and granular form (94.7%). It is believed that the pore space of the granular halloysite nanotubes accommodates phosphorus in addition to physico-chemically bound phosphate at surfaces. The pseudo-first order and pseudo-second order model fitted well the experimental kinetic data for both powder and granular form of halloysite nanotubes. The fit of the Freundlich isotherm model was superior as compared with the Langmuir approach, implying that the halloysite nanotubes are heterogeneous because of multiple surface groups and different pore structures. The two forms of halloysite nanotube tested have the abundant potential for removal of phosphate from agriculture runoff. Additional investigations at the pilot scale are, however, required to draw definite conclusions.

Keywords: phosphate; halloysite nanotubes; adsorption; isotherm; kinetic

1. Introduction

Excessive phosphate discharge from manure, sludge sources, and chemical fertilizer applied to agricultural soils to runoff is the prominent source of water quality deterioration and nutrient enrichment. Heavily phosphate-laden waters impose hazardous risk to aquatic ecosystems [1–4]. Although phosphorus concentrations in runoff from agricultural fields are, in general, below 1 mg L^{-1} , the elimination of phosphorus is considered a crucial environmental sustainability concern to halt rapid degradation of water quality [4–8]. A wide range of phosphorus concentrations has been investigated in phosphorus adsorption studies [1,6,9]. Chemical precipitation, coagulation, ion exchange, biological, and physical treatments have been reported to remove phosphorus from aqueous solutions before it discharges to agricultural runoff [10–12]. Although chemical treatment involving Al, Fe, and Ca is a traditional approach to remove phosphate from wastewater, these methods lead to huge sludge treatment and disposal problems [13]. Physical treatment containing electro dialysis, reverse osmosis, and adsorption seem to be highly promising as compared to chemical treatments to remove phosphate from aqueous solutions [14]. However, except adsorption, most of these methods involve high capital cost with recurring expenses, which are not suitable for many parts of the world [15–18]. Several adsorbents have been investigated in various studies for the removal of phosphate from aqueous solution such as nanoparticles [19,20], nanoscale zero-valent materials [21], activated red mud [22],

biogenetic calcium carbonate minerals [23], hybrid impregnated polymeric sorbent containing hydrated ferric oxide [24], industrial acidified laterite by-product [25], mixture of sand and dolomite [26], slag and fly ash [27], steel slags [28], silicate hybrid materials [29], schwertmannite (which is ferric oxyhydroxide sulphate) [30], and volcanic rocks [31]. Nanoparticle clay mineral receives much more attention among the natural adsorbents due to the high specific surface area, high adsorption rates compared to other adsorbents, low toxicity, easy operation, and, to some extent, cost-effectiveness. The potential of clay materials (halloysite) to remove both anionic and cationic pollutants has been reported [19,32–34]. In recent studies, it was found that halloysite of different chemical and mineralogical composition can be used as an adsorbent and pollution remediation material [35].

Halloysite is a widespread clay mineral in soils and weathered rocks that appears in a variety of particle configuration and hydration states [19,36,37]. Though halloysite particles occur in a variety of morphologies, the dominant morphology is tubular form [19]. Halloysite nanotubes (HNTs) are formed as a result of strain caused by lattice mismatch between adjacent silicon dioxide and aluminum oxide layers. Chemically tubular halloysite can terminate from deformation of platy kaolinite ($\text{Al}_2\text{SiO}_5(\text{OH})_4 \cdot 2\text{H}_2\text{O}$), or it is derived from crystallization of Micas and Feldspar [19,38,39].

HNTs were selected as a compelling candidate for removal of phosphate, and it can be fabricated in a diversity of shapes and varied lattice planes [20]. Despite the tubular shape of HNTs that contribute to adsorption capacity, the interlayer is scarcely accessible for adsorption of ion and molecules. Therefore, application of the modified granular form of HNTs should be considered to improve the adsorption of HNTs [40]. Granular HNTs might have a higher or lower adsorption capacity as compared to the powder form. Theoretical calculations demonstrate that the aggregation of nanotubes leads to a specific reduction in surface area, but at the same time the pore volume is enlarged due to interstices trapped in the aggregated nanotubes [41].

However, no information is available on the adsorptive interactions between phosphate in the aqueous system and HNTs in the aggregated form. Therefore, the objectives of this study were: (1) to examine the characteristics of the HNTs, (2) to investigate the phosphate sorption capacity of HNTs under a batch adsorption setup, (3) to determine kinetics of the adsorption reaction onto HNTs, and (4) to predict the adsorption process by using isotherm models.

2. Materials and Methods

2.1. Adsorbent Characterizations and Preparations

All HNT material used in this study was provided by Durtec Company (Neubrandenburg, Germany). Granular HNT was prepared through compaction employing an EIRICH machine; water was used as a reagent. The size of investigated HNT grains was between 4–6 mm. The HNTs were also characterized by scanning electron microscopy (SEM) to study morphology, size, and elemental composition (Figure 1). The chemical composition and specific surface area of the HNTs was determined by X-ray Fluorescence (XRF) spectrometry and N_2 gas BET analyses using a thermo Sorptomatic 1990 Analyzer (Thermo Fisher Scientific, Milan, Italy).

All chemicals used in this experiments for preparing phosphate solutions and for analyzing adsorbed phosphate, such as KH_2PO_4 , $\text{C}_6\text{H}_8\text{O}_6$, $(\text{NH}_4)_6\text{Mo}_7\text{O}_{24} \cdot 4\text{H}_2\text{O}$, $(\text{SbO})\text{K}(\text{C}_4\text{H}_4\text{O}_6) \cdot 1/2\text{H}_2\text{O}$, H_2SO_4 were analytical reagent grade chemicals from Carl Roth (Karlsruhe, Germany). The varying concentrations of phosphate solution for adsorption experiments were prepared by diluting the stock solution (1000 mg L^{-1} phosphate).

The determination of inorganic phosphate in aqueous solution is based on the reaction of the phosphate ions with the acidic molybdate reagent producing a phosphomolybdate complex. This complex is reduced to a favourably coloured blue compound (Molybdenum blue method) [42].

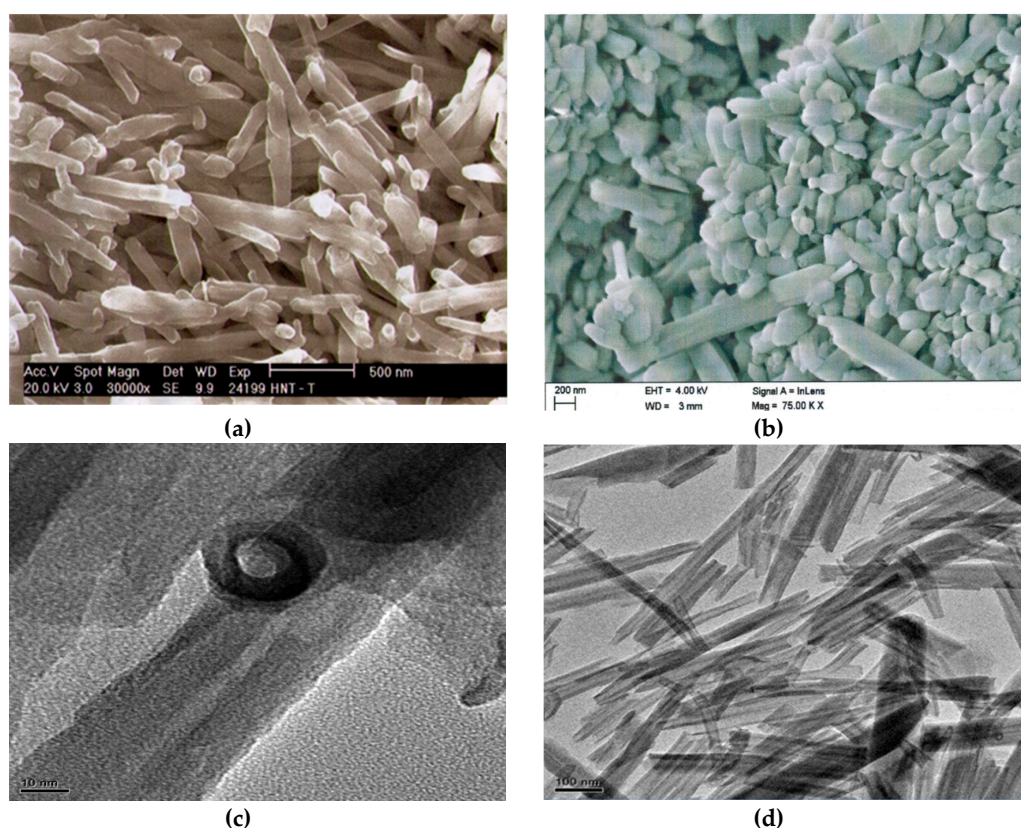


Figure 1. Scanning electron microscope images of halloysite nanotubes (a) HNT-MF4; (b) HNT-MF2; (c) and (d) HNT-MF7.

2.2. Classical Batch Experiments

The classical batch experiment was conducted by agitating 4 g of each adsorbent with 100 mL of phosphate solution of known concentration ranging from 1 mg L⁻¹ to 100 mg L⁻¹ in plastic acid-washed polypropylene bottles (adsorbent:solution ratio, 1:25 g:mL). The batch containers were shaken using a horizontal shaker with the speed of 200 rpm to homogenize the samples and to accelerate the adsorption at a temperature of 22 ± 1 °C and a natural pH (7.014 ± 0.09). At the end of equilibrium time (24 h), the mixtures were filtered through 0.45 µm nylon mesh and the concentration of residual phosphate at equilibrium time was determined by the photometric method (Molybdenum blue method) and a spectrophotometer (Specord 40, Analytik Jena AG, Jena, Germany) at 850 nm [42]. Each experiment was conducted triplicate to check the repeatability of the experimental data, and data represent the mean value of the individual results. The variance in the data of repetition was consistently less than 5%. The amount of phosphate adsorbed at time *t* and the adsorbed amount *q_t* were calculated from the mass balance equation:

$$q_t = (C_0 - C_t) \times \frac{V}{M} \quad (1)$$

where *C₀* is the initial concentration of phosphate in contact with halloysite nanotubes, *C_t* is the mass concentration of phosphate in the aqueous phase at time *t* and *q_t* is the amount of adsorbed phosphate per unit mass of HNTs (mg kg⁻¹), *M* is dry mass of the adsorbent (kg), and *V* the volume of solution (L).

2.3. Kinetic Experiments and Data Presentations

The kinetic experiments for phosphate adsorption onto powder and aggregated form of HNTs were carried out in KH₂PO₄ aqueous solution at an initial phosphate concentration of 20 mg L⁻¹

at room temperature of $22 \pm 1^\circ\text{C}$ under constant and regular agitation using a magnetic stirrer (adsorbent:solution ratio of 1:25 g:mL).

The residual phosphate concentrations in the solution were measured at various contact times ranging from 5 min to 24 h. An aliquot of the solution (5 mL) withdrawn by pipette, and the remaining solids, were separated by filtration (0.45 μm , Nylon Membrane Filters, Carl Roth GmbH, Karlsruhe, Germany). The residual phosphate concentration was measured using the molybdenum blue method as described above [42].

2.4. Kinetic Experiments and Data Presentations

Several models have been proposed to investigate the mechanism of adsorption onto several HNTs [19,21].

In order to evaluate the kinetic adsorption parameters, mathematical models including pseudo-first order (Equation (2)) and pseudo-second order (Equation (3)) equations were used to analyze the experimental data of phosphate adsorption onto HNTs. The equations are expressed as:

$$q_t = q_e \left(1 - e^{-k_1 t}\right), \quad (2)$$

$$q_t = \frac{q_e^2 k_2 t}{1 + k_2 t q_e} \quad (3)$$

where q_t is the amount of adsorbed phosphate at time t , q_e is the amount of adsorbed phosphate at equilibrium time (both in mg kg^{-1}), and k_1 and k_2 are the pseudo-first order rate constant of adsorption (h^{-1}) and the pseudo-second order rate constant of adsorption ($\text{kg mg}^{-1} \text{h}^{-1}$) respectively.

To evaluate isotherm parameters, non-linear isotherm models were fitted to the equilibrium adsorption data. In order to estimate adsorption constants that indicate the adsorption capacity and affinity of the adsorbents, the Langmuir (Equation (4)) and Freundlich (Equation (5)) adsorption isotherms were applied to the data. The isotherm equations have been optimized using the root mean square errors (RMSE).

The equations are expressed as a non-linear function as follows:

$$q_e = \frac{K_L Q C_e}{1 + K_L C_e} \quad (4)$$

$$q_e = K_F C_e^n \quad (5)$$

where q_e is the amount of adsorbed phosphate at equilibrium (mg kg^{-1}), C_e correspond to the equilibrium concentration of phosphate in the solution (mg L^{-1}), Q represents the Langmuir parameter, which is associated with the adsorption density (mg kg^{-1}) and K_L represents the Langmuir coefficient of adsorption energy (L mg^{-1}) and K_F is the Freundlich coefficients expressing the adsorption energy ($\text{mg}^{(1-n)} \text{L}^n \text{kg}^{-1}$), while n is the Freundlich constant representing the adsorption intensity (dimensionless).

3. Results and Discussions

3.1. Morphology and Characterization of HNTs

Table 1 represents the structural characteristics of HNTs from Durtec GmbH, Neubrandenburg, Germany. As expected, the Al_2O_3 content was more magnificent than Fe_2O_3 . Surface characterization depicts that the specific surface area of HNTs ranges from 25 to 35 $\text{m}^2 \text{g}^{-1}$, which is principally appealing for phosphate adsorption. Chemical analysis of HNTs reveals that the amount of Fe_2O_3 is up to 23%. This observation suggests that Fe oxides like hematite and maghemite are associated and/or the partial substitution of Fe^{3+} for Al^{3+} in the octahedral sheet [19,36]. However, further work is needed to better understand HNTs and their properties.

Table 1. Characteristic of the halloysite nanotubes (HNT) powder materials.

Adsorbent	Al ₂ O ₃ (%)	Fe ₂ O ₃ (%)	Specific Surface Area (m ² g ⁻¹)	Morphology				
				Length (μm)	Diameter (nm)		Aspect Ratio	Grain Size
					Inner	Outer		
HNT-MF2	25.0	23.0	35	0.3–1.0	25	120	8	<2 μm
HNT-MF4	37.5	0.4	25	0.6–1.2	20	100	10	<7 μm
HNT-MF7	35.9	1.3	25	0.5–3.5	15	60	30	<7 μm

Joussein et al. [19,29] proposed that morphological variability of halloysite is attributed to various factors including crystal structure, the degree of alteration, chemical composition, and the effects of dehydration. SEM image of HNTs illustrates tubular morphology with different lengths, covering a range from 0.3 to 3.5 μm and the diameter varies from 15 nm to 120 nm, which explains the mesoporous (2–50 nm) and even macroporous scale (>50 nm) [36,37].

3.2. Phosphate Adsorption Kinetics

Principally, the kinetics of phosphate adsorption by HNTs illustrates two different steps of adsorption with different slopes. The adsorption dynamic is characterized by a fast first phase (first 4 h of the experiment) in which 50% of the final amount is adsorbed onto HNTs. The second step corresponds to slower kinetics reaching maximum adsorption at a constant rate beyond 18 h of the experiment (Figure 2). The data indicate that the equilibrium is attained at 24 h. The shaking time for the equilibrium tests was chosen accordingly. A 24 h kinetic experiment appears to be adequate to reach equilibrium, which is in agreement with prior studies [1]. Differences in the temporal dynamic can be attributed to less accessible adsorption site of phosphate and a limited diffusion process in case of granular HNTs. Among studied adsorbents, the amount of phosphate adsorbed on HNT-MF4 (G) (549 mg kg⁻¹, 94.7%) was much higher than the values obtained for all other adsorbents at the same interaction time of 24 h.

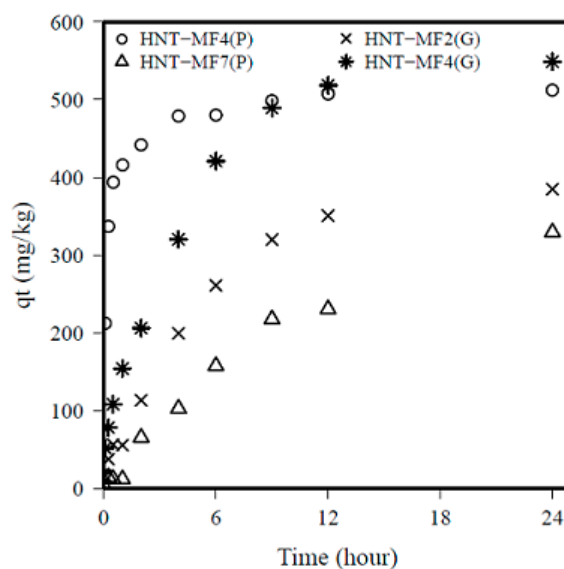


Figure 2. Kinetic experiments for the adsorption of phosphate onto halloysite nanotubes (HNT) material in powder and granular form.

To get more comprehension of the kinetics of phosphate adsorption onto HNTs, different models were fitted to the experimental data. The pseudo-first and pseudo-second order equations were applied in this study, and the parameter values for the kinetic experiment as acquired are reported in Table 2. For all HNTs, the calculated equilibrium capacity values were very close to the experimentally determined values (q_e). The k_1 and k_2 represent the steepness of the curve and describe the rate of

phosphate uptake. From Table 2 it is evident that the adsorption of phosphate onto HNT-MF4(P) is faster than onto the other HNTs. In powder form, the sorption sites of the HNTs are instantly accessible. In general, excellent fits ($R^2 > 0.90$, Table 2) for all HNTs were observed indicating that both kinetic models are applicable. All adsorbent favorably adsorb phosphate efficiently.

Table 2. Pseudo-first and second order parameter values of phosphate adsorption onto different halloysite nanotubes.

Model		Adsorbent Halloysite Nanotubes			
		HNT-MF2 (G)	HNT-MF4 (P)	HNT-MF7 (P)	HNT-MF4 (G)
Pseudo-first order	q_e experiment	384.5	511.6	329.5	549.0
	q_e model	369.9	472.1	328.5	541.1
	K_1	0.19	5.25	0.087	0.256
	RMSE	440.1	1459	143.9	1077
	R^2	0.98	0.87	0.99	0.99
Pseudo-second order	q_e model	384.6	492.3	331.9	565.6
	K_2	0.0004	0.016	0.0001	0.0004
	RMSE	260.1	251.8	136.4	589.6
	R^2	0.98	0.97	0.99	0.98

For the mentioned HNTs (HNT-MF4), q_e values as derived from the pseudo-first order equation are 541.1 mg kg^{-1} and 472.1 mg kg^{-1} for granular form and powder form, respectively indicating a slightly higher adsorption capacity (around 10%) for the granular form at time of equilibrium, although the rate of phosphate uptake of the powder form was higher than that of the granular form at early stages of the experiments ($k_1 = 5.25$ vs. 0.256 h^{-1}) (Figure 3).

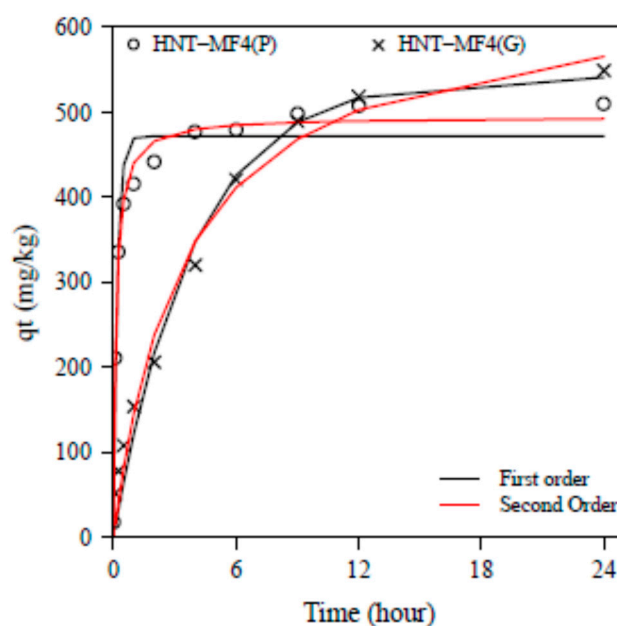


Figure 3. Phosphate adsorption kinetic data and optimized model equations for powder HNT-MF4(P) and granular form of HNT-MF4(G).

3.3. Adsorption Isotherms

Analysis of the relationship between the adsorption capacity of the materials (HNTs) and different phosphate concentrations at equilibrium was performed using the equations of Langmuir (Equation (3)) and Freundlich (Equation (4)). The isotherm plots of the equilibrium adsorption of phosphate are graphically presented in Figure 4, and the parameters values derived from the isotherm models and

the parameters of determination are demonstrated in Table 3. It was found that among the tested materials, adsorption onto the granular form of HNTs was more pronounced than onto powder form. Freundlich equation relatively better describes the adsorption of phosphate onto halloysite nanotubes as indicated by the greater value of R^2 (Table 3).

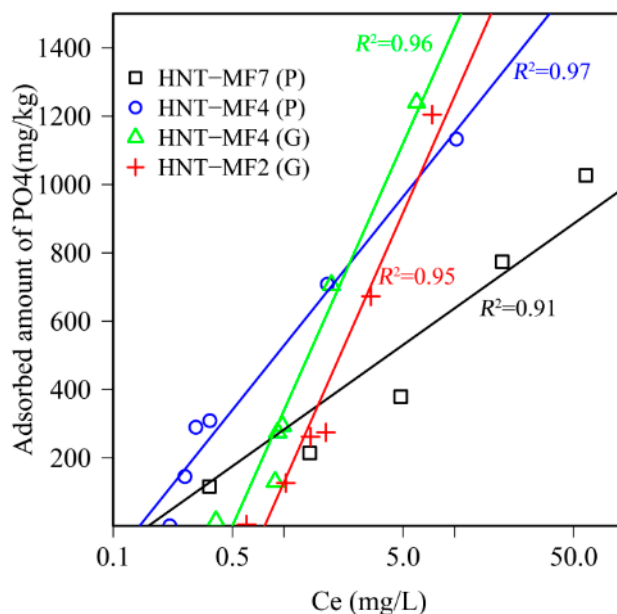


Figure 4. Adsorption isotherms of phosphate for adsorbents HNT-MF4 (P), HNT-MF2 (P), and HNT-MF7 (P).

Table 3. Adsorption Freundlich and Langmuir isotherm data.

Adsorbent	Freundlich				Langmuir			
	K_F	n_F	RMSE	R^2	K_L	Q_L	RMSE	R^2
HNT-MF2(G)	380	0.934	112	0.982	0.918	184	438	0.978
HNT-MF4(P)	334	0.848	203	0.977	0.865	61.2	621	0.798
HNF-MF4(G)	415	0.968	153	0.983	0.937	204	215	0.966
HNT-MF7(P)	207	0.404	311	0.964	0.564	59.4	976	0.727

Nevertheless, in the case of HNT-MF2(G) and HNT-MF4(G), systems follow both Freundlich and Langmuir type adsorption isotherms. The results confirm that the Freundlich adsorption capacity, K_F , of HNT-MF4 (P) is larger (415 L kg^{-1} ; R^2 : 0.983 for HNT-MF4 (G) and 380 L kg^{-1} ; R^2 : 0.982 for HNT-MF2 (G) as compared to that of other adsorbents (345 L kg^{-1} ; R^2 : 0.977 for HNT-MF7 (P) and 207 L kg^{-1} ; R^2 : 0.964 for HNT-MF4 (P)) (Table 3).

The Freundlich constant, n , can be considered a measure of deviation from linearity of adsorption. If $n = 1$ the adsorption is linear, indicating that the adsorption sites are homogenous in energy and no interaction occurs between the adsorbed species [43]. The results revealed that the n values for all adsorbents were less than unity (Table 3), which indicates that increased adsorption can modify the adsorbent and that a chemical rather than physical adsorption was dominant [44,45].

4. Conclusions

The mechanism of phosphate adsorption onto the powder and granular forms of halloysite nanotubes was studied via diffusion and batch experiments. Both powder and granular halloysite nanotubes are adequate of removing phosphate from agricultural runoff. At equilibrium time, the granular form of halloysite nanotubes had a slightly higher adsorption capacity than the powder form. We postulate that the pore volume as formed by the production of grains can accommodate

phosphate anions in addition to the adsorbed amount at solid surfaces. Adsorption of phosphate onto granular halloysite nanotubes took place primarily at active sites of the surface area followed by a slow diffusion into the inner structure of the grains. The Freundlich isotherm model provided a superior fit to data indicating the irregular internal morphology of halloysite nanotubes particles and interrupted placement of the layers. The lab-scale phosphate adsorption onto halloysite nanotubes offers interesting perspectives; however, the use of the halloysite nanotubes for phosphate-laden agricultural runoff requires more investigations deploying real runoff, which also contains dissolved and particulate organic matter and clay minerals possibly altering adsorption behavior. Besides, clogging of filter materials in a flow-through-set-up is a severe problem and may be considered additionally in future studies [46].

Author Contributions: H.S. conducted the research (data collection, calculation, and analysis), reviewed the literature, and drafted the manuscript; E.A. updated and revised the manuscript; J.S. analyze and characterize the halloysite nanotubes; B.L. developed the idea, supervised the study and thoroughly revised the article. All authors approved the final version of this article.

Funding: This research was funded by the German Federal Ministry of Education and Research (BMBF) under PhosWaM—from source to sea—Integrated phosphorus and water resources management for sustainable water protection, grant number 64130151.

Conflicts of Interest: The authors declare no conflict of interest.

References

1. Tabbara, H. Phosphorus loss to runoff water twenty-four hours after application of liquid swine manure or fertilizer. *J. Environ. Qual.* **2003**, *32*, 1044–1052. [[CrossRef](#)] [[PubMed](#)]
2. Tarkalson, D.D.; Mikkelsen, R.L. Runoff Phosphorus Losses as Related to Phosphorus Source, Application Method, and Application Rate on a Piedmont Soil. *J. Environ. Qual.* **2004**, *33*, 1424–1430. [[CrossRef](#)] [[PubMed](#)]
3. Daverede, I.C.; Kravchenko, A.N.; Hoelt, R.G.; Nafziger, E.D.; Bullock, D.G.; Warren, J.J.; Gonzini, L.C. Phosphorus Runoff from Incorporated and Surface-Applied Liquid Swine Manure and Phosphorus Fertilizer. *J. Environ. Qual.* **2004**, *33*, 1535–1544. [[CrossRef](#)]
4. Hart, M.R.; Quin, B.F.; Nguyen, M.L. Phosphorus Runoff from Agricultural Land and Direct Fertilizer Effects. *J. Environ. Qual.* **2004**, *33*, 1954–1972. [[CrossRef](#)] [[PubMed](#)]
5. Boesch, D.F.; Brinsfield, R.B.; Magnien, R.E. Chesapeake Bay eutrophication: Scientific understanding, ecosystem restoration, and challenges for agriculture. *J. Environ. Qual.* **2001**, *30*, 303–320. [[CrossRef](#)]
6. Márquez-Pacheco, H.; Hansen, A.M.; Falcón-Rojas, A. Phosphorous control in a eutrophied reservoir. *Environ. Sci. Pollut. Res.* **2013**, *20*, 8446–8456. [[CrossRef](#)] [[PubMed](#)]
7. Duranceau, S.J.; Biscardi, P.G.; Barnhill, D.K. Screening the toxicity of phosphorous-removal adsorbents using a bioluminescence inhibition test. *Environ. Toxicol.* **2016**, *31*, 489–495. [[CrossRef](#)] [[PubMed](#)]
8. Southam, D.C.; Lewis, T.W.; McFarlane, A.J.; Johnston, J.H. Amorphous calcium silicate as a biosorbent for phosphate. *Curr. Appl. Phys.* **2004**, *4*, 355–358. [[CrossRef](#)]
9. Lewis, W.M.; Wurtsbaugh, W.A.; Paerl, H.W. Rationale for control of anthropogenic nitrogen and phosphorus to reduce eutrophication of inland waters. *Environ. Sci. Technol.* **2011**, *45*, 10300–10305. [[CrossRef](#)] [[PubMed](#)]
10. Farmer, A.M. Reducing phosphate discharges: The role of the 1991 EC urban wastewater treatment directive. *Water Sci. Technol.* **2001**, *44*, 41–48. [[CrossRef](#)]
11. Jones, E.V. *Phosphorus in Environmental Technologies: Principles and Applications*; IWA Publishing: London, UK, 2004; ISBN 9781843390015.
12. Shilton, A.N.; Elmetri, I.; Drizo, A.; Pratt, S.; Haverkamp, R.G.; Bilby, S.C. Phosphorus removal by an “active” slag filter—a decade of full scale experience. *Water Res.* **2006**, *40*, 113–118. [[CrossRef](#)] [[PubMed](#)]
13. Zhang, Y.; Gao, R.; Liu, M.; Yan, C.; Shan, A. Adsorption of modified halloysite nanotubes in vitro and the protective effect in rats exposed to zearalenone. *Arch. Anim. Nutr.* **2014**, *68*, 320–335. [[CrossRef](#)] [[PubMed](#)]
14. Yao, Y.; Gao, B.; Inyang, M.; Zimmerman, A.R.; Cao, X.; Pullammanappallil, P.; Yang, L. Removal of phosphate from aqueous solution by biochar derived from anaerobically digested sugar beet tailings. *J. Hazard. Mater.* **2011**, *190*, 501–507. [[CrossRef](#)] [[PubMed](#)]

15. Gupta, V.K.; Carrott, P.J.M.; Ribeiro Carrott, M.M.L. Suhas Low-Cost adsorbents: Growing approach to wastewater treatment a review. *Crit. Rev. Environ. Sci. Technol.* **2009**, *39*, 783–842. [[CrossRef](#)]
16. Johansson Westholm, L. Substrates for phosphorus removal—Potential benefits for on-site wastewater treatment? *Water Res.* **2006**, *40*, 23–36. [[CrossRef](#)] [[PubMed](#)]
17. Hylander, L.D.; Kietlińska, A.; Renman, G.; Simán, G. Phosphorus retention in filter materials for wastewater treatment and its subsequent suitability for plant production. *Bioresour. Technol.* **2006**, *97*, 914–921. [[CrossRef](#)] [[PubMed](#)]
18. Cucarella, V.; Zaleski, T.; Mazurek, R.; Renman, G. Effect of reactive substrates used for the removal of phosphorus from wastewater on the fertility of acid soils. *Bioresour. Technol.* **2008**, *99*, 4308–4314. [[CrossRef](#)] [[PubMed](#)]
19. Joussein, E.; Petit, S.; Churchman, J.; Theng, B.; Righi, D.; Delvaux, B. Halloysite clay minerals—A review. *Clay Miner.* **2005**, *63*, 383–426. [[CrossRef](#)]
20. Prashantha Kumar, T.K.M.; Mandlimath, T.R.; Sangeetha, P.; Revathi, S.K.; Ashok Kumar, S.K. Nanoscale materials as sorbents for nitrate and phosphate removal from water. *Environ. Chem. Lett.* **2018**, *16*, 389–400. [[CrossRef](#)]
21. Cataldo, S.; Lazzara, G.; Massaro, M.; Muratore, N.; Pettignano, A.; Riela, S. Functionalized halloysite nanotubes for enhanced removal of lead(II) ions from aqueous solutions. *Appl. Clay Sci.* **2018**, *156*, 87–95. [[CrossRef](#)]
22. Baraka, A.M.; El-Tayieb, M.M.; Shafai, M.E.; Mohamed, N.Y. Sorptive Removal of Phosphate from Wastewater Using Activated Red Mud 1. *Aust. J. Basic Appl. Sci.* **2012**, *6*, 500–510.
23. Liu, Q.; Guo, L.; Zhou, Y.; Dai, Y.; Feng, L.; Zhou, J.; Zhao, J.; Liu, J.; Qian, G. Phosphate adsorption on biogenetic calcium carbonate minerals: Effect of a crystalline phase. *Desalin. Water Treat.* **2012**, *47*, 78–85. [[CrossRef](#)]
24. You, X.; Guaya, D.; Farran, A.; Valderrama, C.; Cortina, J.L. Phosphate removal from aqueous solution using a hybrid impregnated polymeric sorbent containing hydrated ferric oxide (HFO). *J. Chem. Technol. Biotechnol.* **2016**, *91*, 693–704. [[CrossRef](#)]
25. Glocheux, Y.; Pasarín, M.M.; Albadarin, A.B.; Mangwandi, C.; Chazarenc, F.; Walker, G.M. Phosphorus adsorption onto an industrial acidified laterite by-product: Equilibrium and thermodynamic investigation. *Asia-Pac. J. Chem. Eng.* **2014**, *9*, 929–940. [[CrossRef](#)]
26. Prochaska, C.A.; Zouboulis, A.I. Removal of phosphates by pilot vertical-flow constructed wetlands using a mixture of sand and dolomite as substrate. *Ecol. Eng.* **2006**, *26*, 293–303. [[CrossRef](#)]
27. Ragheb, S.M. Phosphate removal from aqueous solution using slag and fly ash. *HBRC J.* **2013**, *9*, 270–275. [[CrossRef](#)]
28. Barca, C.; Gérente, C.; Meyer, D.; Chazarenc, F.; Andrès, Y. Phosphate removal from synthetic and real wastewater using steel slags produced in Europe. *Water Res.* **2012**, *46*, 2376–2384. [[CrossRef](#)]
29. Zhang, J.; Shen, Z.; Mei, Z.; Li, S.; Wang, W. Removal of phosphate by Fe-coordinated amino-functionalized 3D mesoporous silicates hybrid materials. *J. Environ. Sci.* **2011**, *23*, 199–205. [[CrossRef](#)]
30. Eskandarpour, A.; Sassa, K.; Bando, Y.; Okido, M.; Asai, S. Magnetic Removal of Phosphate from Wastewater Using Schwertmannite. *Mater. Trans.* **2006**, *47*, 1832–1837. [[CrossRef](#)]
31. Fetene, Y. Design Phosphate Removal Technology using Volcanic Rocks: Kinetics and Equilibrium Studies. *Int. J. Eng. Res. Technol.* **2015**, *4*, 155–162. [[CrossRef](#)]
32. Mallikarjun, S.D.; Mise, S.R. A Batch Study of P Hosphate Adsorption Characteristics on Clay Soil. *Int. J. Res. Eng. Technol.* **2013**, *1*, 338–342.
33. Dong, Y.; Liu, Z.; Chen, L. Removal of Zn(II) from aqueous solution by natural halloysite nanotubes. *J. Radioanal. Nucl. Chem.* **2012**, *292*, 435–443. [[CrossRef](#)]
34. Cataldo, S.; Muratore, N.; Orecchio, S.; Pettignano, A. Enhancement of adsorption ability of calcium alginate gel beads towards Pd(II) ion. A kinetic and equilibrium study on hybrid Laponite and Montmorillonite-alginate gel beads. *Appl. Clay Sci.* **2015**, *118*, 162–170. [[CrossRef](#)]
35. Matusik, J. Halloysite for Adsorption and Pollution Remediation. *Dev. Clay Sci.* **2016**, *7*, 606–627. [[CrossRef](#)]
36. Yuan, P.; Tan, D.; Annabi-Bergaya, F. Properties and applications of halloysite nanotubes: Recent research advances and future prospects. *Appl. Clay Sci.* **2015**, *112–113*, 75–93. [[CrossRef](#)]
37. Pasbakhsh, P.; Churchman, G.J.; Keeling, J.L. Characterisation of properties of various halloysites relevant to their use as nanotubes and microfibre fillers. *Appl. Clay Sci.* **2013**, *74*, 47–57. [[CrossRef](#)]

38. Furumi, S.; Uchikoshi, T.; Shirahata, N.; Suzuki, T.S.; Sakka, Y. Aqueous dispersions of carbon nanotubes stabilized by zirconium acetate. *Nanosci. Nanotechnol.* **2009**, *9*, 662–665. [[CrossRef](#)]
39. Singh, B.; Gilkes, R.J. An electron optical investigation of the alteration of kaolinite to halloysite. *Clays Clay Miner.* **1992**, *40*, 212–229. [[CrossRef](#)]
40. Yuan, P.; Thill, A.; Bergaya, F. *Nanosized Tubular Clay Minerals: Halloysite and Imogolite*; Elsevier: Amsterdam, The Netherlands, 2016.
41. Zhang, S.; Shao, T. The Impacts of Aggregation and Surface Chemistry of Carbon Nanotubes on the Adsorption of Synthetic Organic Compounds. *Environ. Sci. Technol.* **2009**, *43*, 5719–5725. [[CrossRef](#)]
42. Murphy, J.; Riley, J.P. A modified single solution method for the determination of phosphate in nature waters. *Anal. Chem. ACTA* **1962**, *27*, 31–36. [[CrossRef](#)]
43. Panuccio, M.R.; Sorgonà, A.; Rizzo, M.; Cacco, G. Cadmium adsorption on vermiculite, zeolite and pumice: Batch experimental studies. *J. Environ. Manag.* **2009**, *90*, 364–374. [[CrossRef](#)] [[PubMed](#)]
44. Jiang, J.Q.; Cooper, C.; Ouki, S. Comparison of modified montmorillonite adsorbents Part I: Preparation, characterization and phenol adsorption. *Chemosphere* **2002**, *47*, 711–716. [[CrossRef](#)]
45. Alemayehu, E.; Lennartz, B. Adsorptive removal of nickel from water using volcanic rocks. *Appl. Geochem.* **2010**, *25*, 1595–1602. [[CrossRef](#)]
46. Loganathan, P.; Vigneswaren, S.; Kandasamy, J.; Bolan, N.S. Removal and recovery of phosphate from water using sorption. *Environ. Sci. Technol.* **2014**, *44*, 847–907. [[CrossRef](#)]



© 2019 by the authors. Licensee MDPI, Basel, Switzerland. This article is an open access article distributed under the terms and conditions of the Creative Commons Attribution (CC BY) license (<http://creativecommons.org/licenses/by/4.0/>).